Nanoscale

Accepted Manuscript

RSC Publishing

www.rsc.org/nanoscale

Registered Charity Number 207890

Journal Name RSCPublishing

ARTICLE

Light Extraction Enhancement with Radiation Pattern Shaping of LEDs By Waveguiding Nanorods with Impedance-Matching Tips

Cite this: DOI: 10.1039/x0xx00000x

Received 00th January 2012,
Accepted 00th January 2012

DOI: 10.1039/x0xx00000x

www.rsc.org/

Yu-Hsuan Hsiao, Cheng-Ying Chen, Li-Chuan Huang, Guan-Jhong Lin, Der-Hsien Lien, Jian-Jang Huang, and Jr-Hau He*

Syringe-like ZnO nanorods (NRs) were fabricated on InGaN/GaN light emitting diodes (LEDs) by a hydrothermal method. Without sacrificing the electrical performances of LEDs, syringe-like NRs can enhance light extraction capability by 10.5% at 20 mA and shape the radiation profile with a view angle collimated from 136° to 121°. By performing optical experiments and simulation, it is found that the superior light extraction efficiency with a more collimated radiation pattern is attributed to the waveguiding effect of NRs and the mitigation of abrupt index change by the tapered ends of syringe-like ZnO NRs. This work demonstrates the importance of nanostructure morphology to LED performances and provides the architecture design guidelines of nanostructures to a variety of optical devices.

Introduction

Having widely tunable emission wavelengths, nitride-based LEDs act as promising candidates in solid-state lighting, signaling, and large displays. However, the external quantum efficiency of the GaN-based LEDs is still low in conventional $In_xGa_{1-x}N$/GaN multiple quantum well (MQW) structures due to unsatisfactory light extraction efficiency.[1]

Low light extraction efficiency is mainly due to the considerable Fresnel loss and total internal reflection loss caused by the large difference in refractive index (*n*) at air/GaN ($n \sim 2.43$) or the air/ITO ($n \sim 2.06$) interfaces.[2] It is unavoidable to experience a severe Fresnel reflection loss at the surface of semiconductor, considering the abrupt interface between the two media. As for the total internal reflection, photons emitted from the MQWs would be reflected from the interface, reabsorbed, and internally confined if the escape angle is larger than the critical angle. Based on Snell's law, the critical angles in LEDs are 54.83° and 29.04° at p-GaN/ITO and ITO/air interface, respectively. Moreover, a variety of LED applications such as pocket lamps, smart phone cameras, and vehicle head lamps are hindered by poor directional emission profiles of conventional $In_xGa_{1-x}N$/GaN MQW LEDs due to a broad radiation pattern.[3] A small view angle is desired for many LED applications. Briefly speaking, it is important to develop high-light-extraction efficiency LEDs with directional radiation profiles for next-generation solid-state lighting devices.

To improve the light extraction of LEDs, various strategies have been proposed to alleviate the total internal reflection and Fresnel reflection. Here are some examples: surface texturing,[4] photonic crystals,[5,6] planar graded-refractive-index antireflection coatings,[7] patterning of sapphire substrates,[8] and sub-microrods for the waveguiding effect.[9] Although the light-extraction enhancement has been obtained *via* these approaches, the directional emission property has not been controlled at the same time. There have been few studies on the light-propagation control through the nanorod (NR) array or photonic crystals.[3,10-12] These methods involve, however, either non-scalable processes or complex, damage-induced fabrications, and can possibly lead to severe electrical degradation. Recently, it has been found that ZnO nanostructures exhibit excellent antireflective properties and in-plane birefringence owing to their moth eye-like structures[13-15] as well as large aspect ratio.[16] Moreover, ZnO NRs have been grown uniformly on a 5-inch Si solar wafer using the hydrothermal process, which is a simple, low-temperature, and scalable process allowing ZnO nanostructures to grow on any substrates regardless of their lattice match or surface chemistry.[14,17] These merits all render the hydrothermally grown ZnO nanostructures readily compatible with the well-developed processes for enhancing the overall efficiency of nitride LEDs without altering the active layer.

In this study, syringe-like ZnO NRs were synthesized on nitride-based LEDs by a hydrothermal method. The LEDs with syringe-like ZnO NRs exhibit an increased extraction efficiency by 10.5% at 20 mA with the view angle improved from 136° to 121°, as compared to the bare LEDs. We experimentally and theoretically demonstrated that better light extraction efficiency and a more collimated radiation pattern are attributed to the waveguiding effect of NRs and the mitigation of abrupt index change by the tapered ends of syringe-like ZnO NRs. Based on the optical experiments and simulation, our findings provide prominent design criteria for the morphology of nanostructures for high-efficiency optical devices.

Experimental

The epitaxial layer of the LEDs followed the conventional growth steps. Nitride-based epitaxial layers were grown on sapphire substrates with c-face orientation by MOCVD technique. The device structure of the InGaN/GaN MQW LEDs were formed by sandwiching nine periods of $In_{0.3}Ga_{0.7}N$ (3 nm)/GaN (17 nm) MQWs between n-type (2.5 μm) and p-type (0.2 μm) GaN layer. ITO was deposited by electron beam evaporation on p-GaN to form transparent ohmic contacts, followed by the deposition of metal electrodes of Ti/Al/Ni/Au on the top surface of ITO and n-GaN. For the employment of ZnO NRs on the device, a 100-nm ZnO seed layer was deposited by electron beam evaporation. The ZnO NRs were fabricated using the hydrothermal method by dipping the samples with seed layers into the solution containing 20 mM of zinc nitrate hexahydrate and 5 cc of ammonia. Through careful control of the growth condition, self-aligned ZnO NRs with tapered tips were formed on the top surface of the LED devices.

Results and discussion

Figure 1 reveals the morphology of the as-fabricated ZnO syringe-like NRs. The cross-sectional scanning electron microscopy (SEM) image is presented in Fig. 1(a), and Fig. 1(b) is the schematic of an individual syringe-like NR. One can see that the syringe-like NR consists of two fragments: the rod-like body and the tapered finish at the top. From the high-magnification SEM image shown in the inset of Fig. 1(a), the gradual decrease in radius of this tapered part can be perceived. The dimensions of the NRs are clarified in Fig. 1(b): average diameter and height of the rod-like bodies are ~120 nm and ~1.75 μm, respectively, and the length of the tapered part is

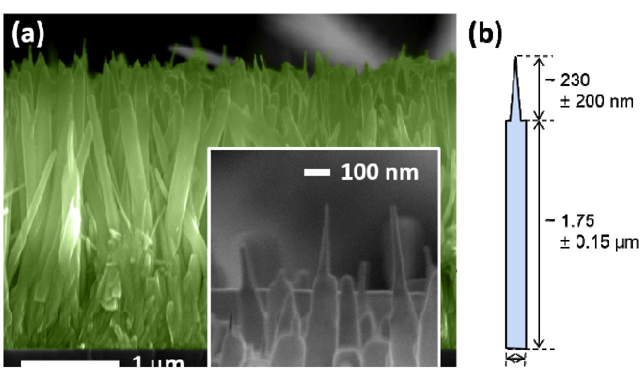

Fig. 1 SEM images of the syringe-like ZnO NRs. The inset in (a) highlights the tapered ending on the top of the NRs. (b) Schematic of a typical syringe-like NR.

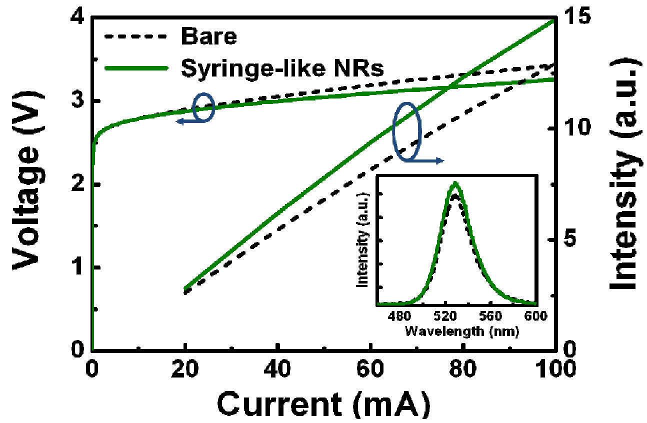

Fig. 2 Typical I-V and L-I characteristics of the bare LEDs and LEDs with syringe-like ZnO NRs. The inset depicts the EL spectra of the LEDs under 20 mA injection current.

230±200 nm. It has been reported that the diameter of ZnO nanostructures is dependent on the solution concentration.[15,18,19] Generally, the shape of ZnO NRs is assumed to relate to a dissolution-recrystallization mechanism. When the OH^- concentration in solution exceeds the critical concentration, the dissolution rate of ZnO increases and the growth rate of ZnO decreases. Accordingly, the syringe-like NRs are fabricated sequentially by alternating the process condition, such as solution concentration during hydrothermal growth.[15] This is one of the advantages of the hydrothermal method: one can alter the configuration of the ZnO nanostructure with ease by controlling growth condition. Furthermore, the process temperature of this solution method is under 100 °C, which is much lower than the fabrication temperature of the host LED and the metal electrode deposition, demonstrating its compatibility to LED processes. We note that other techniques have been utilized to fabricate ZnO NRs, but a higher process temperature is required in these fabrication methods such as metal-organic chemical vapor deposition (MOCVD) (400~500 °C),[20] which can be harmful to the device structure and metal electrodes and lead to degradation of electrical properties of the LED.[21]

The forward current-voltage (I-V) characteristics of the LEDs are presented in Fig. 2. The forward voltage (V_f) under 20 mA injection current are 2.88 and 2.89 V for the LEDs with and without syringe-like ZnO NRs, respectively. The I-V curves are almost identical, indicating that the low-temperature hydrothermal method for ZnO syringe-like NRs does not degrade the electrical properties of the LEDs. In contrast, as the ZnO nanostructure are grown on the nitride LEDs using MOCVD, significant increase in V_f may occur, which is not desired because the overall efficiency of the LED is related to the input electrical power. Figure 2 also demonstrates the relative light output intensity as a function of injection current, and the inset in Fig. 2 reveals the electroluminescence (EL) spectra of two kinds of LEDs measured at 20 mA injection current. After introducing syringe-like ZnO NRs, the peak intensity of the LED is increased by 10.5% and 16.8% at injection currents of 20 and 100 mA, respectively, indicating excellent light extraction characteristics of syringe-like ZnO NRs. Moreover, The external quantum efficiency (EQE) is an important characteristic for revealing the LED performance. The EQE values were obtained by varying the input current and measuring the output light power of the LEDs in an integrating sphere. The EQE of the bare device is 13% at 20 mA. By applying syringe-like ZnO NRs, the EQE achieves 14.4%. The enhanced light extraction can be attributed to the waveguiding effect and tapered tip morphology of the syringe-like ZnO NRs, which will be discussed with experimental and simulation results in the following paragraphs.

To evidence the waveguiding effect of the ZnO NR, some of the NRs were dispersed on a SiO_2/Si substrate and examined by a 532-nm laser with the optical microscope (OM) as an optical coupler. Fig. 3(a) shows the OM image of a single ZnO NR. The laser light was coupled into the NR at the bottom by the objective lens and guided out at the top end, clearly demonstrating the waveguiding characteristics of the NR.

As mentioned earlier, the ZnO nanostructure growth is on the basis of the dissolution/crystallization behavior, which is significantly influenced by the solution concentration. Accordingly, it is hard to have ZnO NRs with the same body length without tapered end as the control sample by the hydrothermal method. In conjunction with experimental results demonstrated earlier, a simulation based on finite-difference time-domain (FDTD) method is carried out to further reveal the light propagation through the syringe-like ZnO NRs. The waveguiding nature of the NRs will be demonstrated in the simulation section, and the importance of the tapered tip of the syringe-like NRs will be distinguished from the flat-end counterpart. In order to simplify the simulation scheme and highlight the waveguiding effect, the NRs are set to be perpendicular to the ITO surface and equally spaced. The diameter and the height of the NR bodies are 130 nm and 1.5 μm, respectively, and the length of the tapered part is 300 nm. Three LEDs with different surface conditions are compared in the simulation: the bare LED, the LEDs with flat-end NRs and syringe-like NRs. The flat-end NRs are constructed by removing the tapered finish of the syringe-like NRs. The monochromatic excitation source is chosen to be at 528.5 nm, matching with the wavelength of the peak emission in the EL spectra at 20 mA injection current. It is sandwiched between a medium of n = 2.43, corresponding to the MQW region surrounded by GaN in the practical LED scheme, and injects light into the NRs at the bottom. A detector is set up at a distance far enough to detect the time-averaged power emitted from the LEDs. Figure 3(b) shows the calculated optical power as a function of time for the three simulation schemes. The showed optical power is normalized with respect to the excitation power. After the excitation source lit up at t = 0, the system would undergo a short period of transient state before reaching the steady state. From the figure, the steady state optical power for the LEDs with flat-end and syringe-like NRs are 3.6% and 8.6% greater than the bare counterpart, respectively.

The electric field inside the surface structures can be visualized in Fig. 3(c)-3(e). These figures depict the transverse electric (TE) field intensity distributions, $|E_y|$, for the LEDs with different surface morphology at steady states. By examining the coloring at the top of Fig. 3(c)-3(e), which indicates the outward field of the LEDs, one can see that the LEDs with surface nanostructures exhibit stronger field intensity. On the other hand, as shown in Fig. 3(c), the strong back reflection occurring at the abrupt surface between the bare

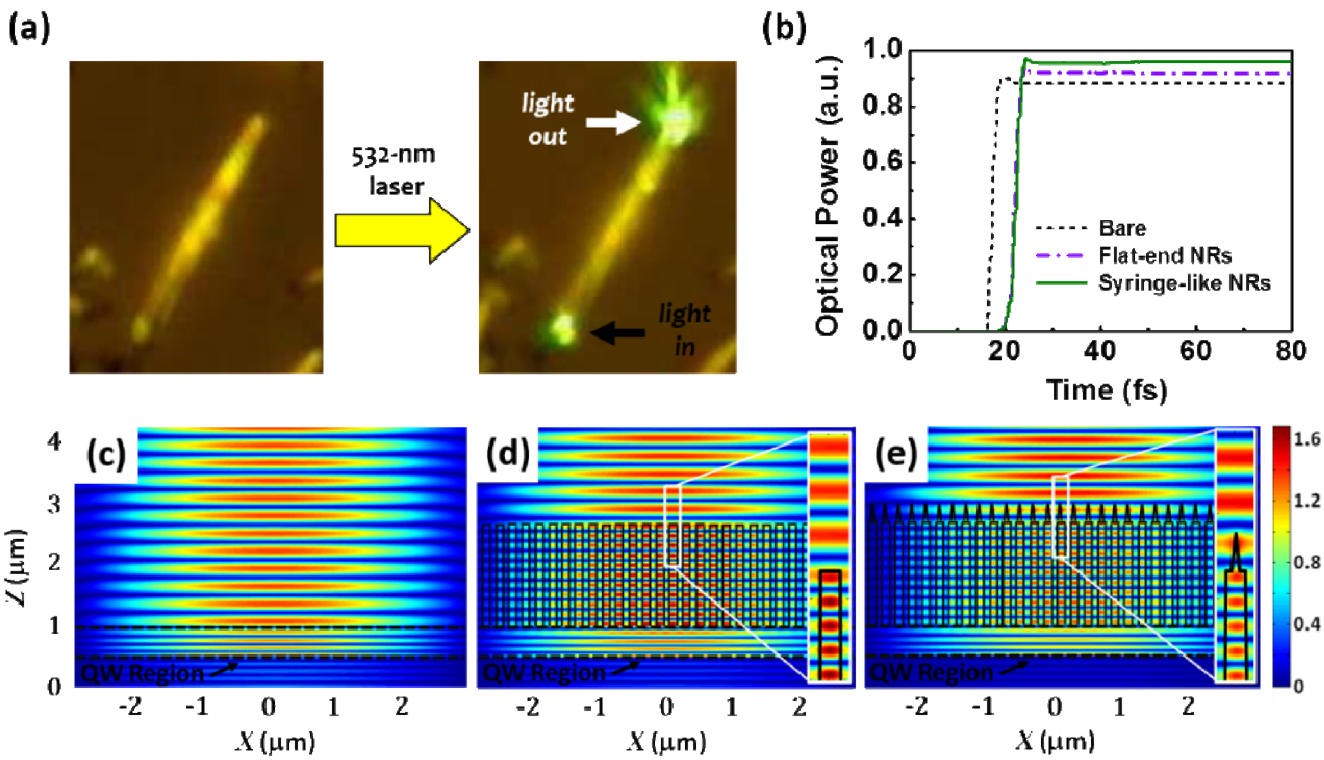

Fig. 3 (a) OM image of the ZnO NR before (left) and after (right) laser illumination. The 532-nm laser was injected into the NR at the bottom end (indicated by black arrow) and extracted out at the top end (white arrow). (b) Calculated optical power as a function of time. (c-e) Time-averaged and normalized TE field distribution near the surface of the LEDs with different surface morphology: (c) bare, (d) flat-end NRs, and (e) syringe-like NRs. The insets in (d) and (e) highlight the ending region of the NRs.

LED and air is observed. One should note that one of the main reasons for the low efficiency of the conventional LEDs is that a great portion of the emitted light from active region is reflected back into the LED and trapped inside due to large refractive index contrast. The employment of the nanostructures effectively reduces such back reflection and ensures better propagation of light by matching the optical impedance at the interface. Furthermore, the syringe-like NRs manifest better light extraction capability than the flat-end counterpart, which has already been illustrated in the steady-state power in Fig. 3(b). The impact of the tapered tip of the syringe-like NRs can be well demonstrated by comparing the electric fields inside the NRs as revealed in the insets of Fig. 3(d) and 3(e). The field inside the flat-end NR is stronger than that inside the syringe-like counterpart because of the reflection induced at the flat-end. As a result, some of the light is trapped in the flat-end NR due to the mismatch in optical impedance of ZnO and air. On the other hand, the tapered finish of the syringe-like NR ensures a good coupling of the traveling wave into air, and thus guarantees a stronger output field. The light extraction enhancement *via* syringe-like ZnO NRs revealed from experimental and simulation investigations can be explained by two steps. Firstly, a major portion of the photons emitted from the MQWs are easily captured by the ZnO NRs interfacing with the ITO top contact, rather than escaping at the ITO/air interface due to well matched refractive index between ZnO (~2.04) and ITO (~2.06).[9] The captured photons are then guided within the ZnO NRs because the substantial difference in the refractive indices between air and ZnO makes NRs natural waveguides.[22] Secondly, at the top end the diameter of the syringe-like ZnO NRs gradually reduced along the vertical direction, and the tapered tips of ZnO NRs can be viewed as an effective medium with continuous gradient of refractive index. Therefore, the guided photons inside the ZnO NRs can be emitted into air on account of the improved impedance match between air and NRs. Without the tapered-tip morphology, the light would be trapped in the ZnO NRs owing to the large optical impedance difference between air and ZnO. The match of the impedance difference at the interface by gradual change in nanostructure morphology is also supported by the recent results in solar cells.[15,23] For example, Fan *et al.* used anodic alumina oxide as a template to control the growth of Ge nanopillar arrays and demonstrated that introducing small-diameter tips on the large-diameter nanopillars increases the optical absorbance of the Ge nanopillar arrays. Briefly speaking, with syringe-like ZnO NRs, not only the light propagation trajectory is bent towards the vertical direction due to the ZnO NRs but a large number of photons also could easily escape due to the tapered tips of ZnO NRs. Moreover, since the spacing between syringe-like ZnO NRs is minute, the evanescent tail in the lateral direction can be coupled into adjacent NRs and guided upwards instead of fading away.[24]

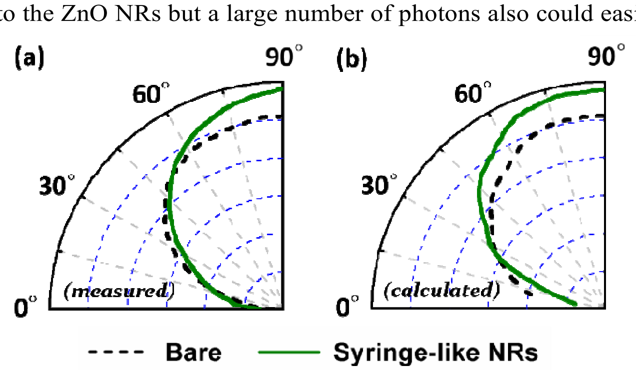

Fig. 4 (a) Measured and (b) calculated far-field radiation patterns of the bare LED and the LED with syringe-like NRs.

Apart from amplifying the output intensity of nitride LEDs (Fig. 2), based on the experimental and simulation observation in light propagation through the ZnO NRs (Fig. 3), the syringe-like NRs are expected to modify the far-field radiation patterns of nitride LEDs. The far-field radiation pattern is the light intensity distribution measured in the angular range of 0-90°. As shown in Fig. 4(a), the bare LED at 20 mA injection current shows a view angle of 136° while the LED with syringe-like NRs exhibits a more collimated radiation pattern, *i.e.* a view angle of 121°. Figure 4(b) is the calculated far-field pattern based on a FDTD method, consistent with experimental results shown in Fig. 4(a). Note that an ideal Lambertian pattern has a view angle of 120°. The wide radiation pattern of the bare LED obtained here can be ascribed to side emission: a large portion of light emitted from the MQW region is reflected by the metal electrode or experience total internal reflection, preventing light from direct emission out of the top surface. After undergoing multiple reflection inside the LED, the light is directed towards periphery and emitted laterally, resulting in a wide radiation pattern.[25] By introducing syringe-like NRs on the surface of LEDs, the generated photons can be collected by the NRs due to the matched optical impedance between ZnO and ITO and then be directed toward vertical direction by the waveguiding effect of the NRs. As a consequence, the side emission is suppressed while the light intensity at normal direction is amplified. This collimated radiation pattern of the LED with syringe-like NRs (Fig. 4) echoes the experimental and simulation results (Fig. 2 and 3). We do note that the present work was done with the LEDs in bare-chip forms. As the LEDs are encapsulated for most commercial applications, the effect of the surface texture should be reconsidered. The investigation is now in progress.

Conclusions

In summary, using a simple, low-temperature and etching-free solution method, syringe-like ZnO NRs grown on nitride-based LEDs efficiently enhance the light extraction by 10.5% at 20 mA and shape the radiation pattern from 136° to 121° without complexly tailoring the configuration of MQW regions. This is ascribed to the waveguiding effect and the creation of smooth refractive index profile at the interface between air and NR layers by the tapered tips of syringe-like ZnO NRs, confirmed by the experiments and optical simulations. The syringe-like ZnO NRs using scalable, cost-effective fabrication technique provide a viable solution for achieving better light extraction and more collimated radiation pattern in the existing solid-state lighting technology.

Acknowledgements

This work was supported by National Science Council of Taiwan (102-2628-M-002-006-MY3 and 101-2221-E-002-115-MY2) and National Taiwan University (10R70823).

Notes and references

Institute of Photonics and Optoelectronics & Department of Electrical Engineering, National Taiwan University, Taipei 10617, Taiwan.
*E-mail: jhhe@cc.ee.ntu.edu.tw

† Footnotes should appear here. These might include comments relevant to but not central to the matter under discussion, limited experimental and spectral data, and crystallographic data.
Electronic Supplementary Information (ESI) available: [details of any supplementary information available should be included here]. See DOI: 10.1039/b000000x/

1 M. Y. Ke, C. Y. Wang, L. Y. Chen, H. H. Chen, H. L. Chiang, Y. W. Cheng, M. Y. Hsieh, C. P. Chen, and J. J. Huang, *IEEE J. Sel. Topics Quantum Electron.*, 2009, **15**, 1242.
2 E. F. Schubert, T. Gessmann and J. K. Kim, in *Kirk-Othmer Encyclopedia of Chemical Technology*, John Wiley & Sons, Inc. 2000.
3 C. H. Ho, D. H. Lien, Y. H. Hsiao, M. S. Tsai, D. Chang, K. Y. Lai, C. C. Sun, and J. H. He, *Appl. Phys. Lett.*, 2013, **103**, 161104.
4 T. Fujii, Y. Gao, R. Sharma, E. L. Hu, S. P. DenBaars and S. Nakamura, *Appl. Phys. Lett.*, 2004, **84**, 855.
5 S. Fan, P. R. Villeneuve, J. D. Joannopoulos and E. F. Schubert, *Phys. Rev. Lett.*, 1997, **78**, 3294.
6 H. W. Huang, C. H. Lin, Z. K. Huang, K. Y. Lee, C. C. Yu and H. C. Kuo, *IEEE Electron Device Lett.*, 2009, **30**, 1152.
7 J. K. Kim, S. Chhajed, M. F. Schubert, E. F. Schubert, A. J. Fischer, M. H. Crawford, J. Cho, H. Kim and C. Sone, *Adv. Mater.*, 2008, **20**, 801.
8 Y. J. Lee, C. H. Chiu, C. C. Ke, P. C. Lin, T. C. Lu, H. C. Kuo and S. C. Wang, *IEEE J. Sel. Topics Quantum Electron.*, 2009, **15**, 1137.
9 K. S. Kim, S. M. Kim, H. Jeong, M. S. Jeong and G. Y. Jung, *Adv. Funct. Mater.*, 2010, **20**, 1076.
10 H. K. Lee, Y. H. Ko, G. S. Raju and J. S. Yu, *Opt. Express*, 2012, **20**, 25058.
11 K. McGroddy, A. David, E. Matioli, M. Iza, S. Nakamura, S. DenBaars, J. S. Speck, C. Weisbuch and E. L. Hu, *Appl. Phys. Lett.*, 2008, **93**, 103502.
12 Y. W. Cheng, K. M. Pan, C. Y. Wang, H. H. Chen, M. Y. Ke, C. P. Chen, M. Y. Hsieh, H. M. Wu, L. H. Peng and J. Huang, *Nanotechnology*, 2009, **20**, 035202.
13 Y. C. Chao, C. Y. Chen, C. A. Lin and J. H. He, *Energy Environ. Sci.*, 2011, **4**, 3436.
14 C. A. Lin, K. Y. Lai, W. C. Lien and J. H. He, *Nanoscale*, 2012, **4**, 6520.
15 L. K. Yeh, K. Y. Lai, G. J. Lin, P. H. Fu, H. C. Chang, C. A. Lin and J. H. He, *Adv. Energy Mater.*, 2011, **1**, 506.
16 C. Y. Chen, J. H. Huang, K. Y. Lai, Y. J. Jen, C. P. Liu and J. H. He, *Opt. Express*, 2012, **20**, 2015.
17 C. A. Lin, D. S. Tsai, C. Y. Chen and J. H. He, *Nanoscale*, 2011, **3**, 1195.
18 L. Vayssieres, *Adv. Mater.*, 2003, **15**, 464.
19 X. Liu, Z. Jin, S. Bu, J. Zhao, and Z. Liu, *J. Am. Ceram. Soc.*, 2006, **89**, 1226.
20 J. Zhong, H. Chen, G. Saraf, Y. Lu, C. K. Choi, J. J. Song, D. M. Mackie and H. Shen, *Appl. Phys. Lett.*, 2007, **90**, 203515.
21 K. K. Kim, S. D. Lee, H. Kim, J. C. Park, S. N. Lee, Y. Park, S. J. Park and S. W. Kim, *Appl. Phys. Lett.*, 2009, **94**, 071118.
22 R. Hauschild and H. Kalt, *Appl. Phys. Lett.*, 2006, **89**, 123107.
23 Z. Fan, R. Kapadia, P. W. Leu, X. Zhang, Y. L. Chueh, K. Takei, K. Yu, A. Jamshidi, A. A. Rathore, D. J. Ruebusch, M. Wu, and A. Javey, *Nano Lett.* 2010, **10**, 3823.
24 L. Zhao, Y. Li, J. Qi, J. Xu and Q. Sun, *Opt. Express*, 2009, **17**, 17136.
25 J. K. Sheu, C. M. Tsai, M. L. Lee, S. C. Shei and W. C. Lai, *Appl. Phys. Lett.*, 2006, **88**, 113505.

ToC

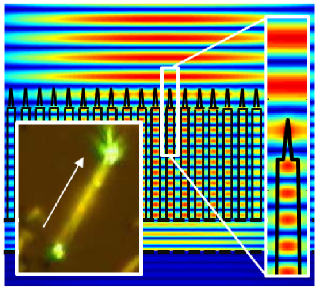

The ZnO nanorods with impedance-matching tips successfully enhance the output of LEDs.